Műszaki Tudományos Közlemények vol. 23. (2025) 80–86.
DOI: Hungarian: https://doi.org/10.33895/mtk-2025.23.11
English: https://doi.org/10.33894/mtk-2025.23.11

# FINITE ELEMENT ANALYSIS OF A RUNNING-SPECIFIC TRANSTIBIAL PROSTHESIS DESIGNED FOR ADDITIVE MANUFACTURING

Krisztina SZŐCS,[1] Erzsébet EGYED-FALUVÉGI[2]

[1] *Sapientia Hungarian University of Transylvania, Faculty of Technical and Human Sciences Targu Mures, Department of Mechanical Engineering, Târgu Mures, Romania, szocs.krisztina@student.ms.sapientia.ro*

[2] *Sapientia Hungarian University of Transylvania, Faculty of Technical and Human Sciences Targu Mures, Department of Mechanical Engineering, Târgu Mures, Romania, faluvegi.erzsebet@ms.sapientia.ro*

**Abstract**

This study explores the application of additive manufacturing in the design and testing of transtibial running prostheses. The research consists of two main phases: design and evaluation. The prosthesis model is created using Autodesk Inventor, incorporating different internal lattice structures—grid, triangular, and zig-zag patterns—optimally suited for 3D printing. These structures aim to balance weight reduction and load-bearing capacity. The model is then subjected to finite element analysis (FEA) using ANSYS software to assess its structural performance under three distinct loading conditions. The analysis examines deformation and stress distribution to determine the most effective internal pattern for maximizing strength while minimizing material usage. Identifying the optimal infill pattern could lead to more efficient manufacturing processes, reducing material and production costs while providing lighter, more comfortable prosthetic solutions for athletes.

**Keywords***: running prosthesis, additive manufacturing, finite element method.*

## 1. Introduction

The history of prosthetic production dates to ancient times. Humanity has always strived to replace lost limbs from the earliest days. Prosthetics provided wearers with the opportunity to return to their daily tasks, offering emotional comfort and a partial restoration of the wholeness tragically lost. Numerous ancient artefacts testify to the long history of prosthetics, yet it was warfare that truly popularized them. Injured soldiers frequently used artificial limbs made predominantly of iron, occasionally of wood. Iron prosthetic arms were in use from ancient times through the Middle Ages. Though rudimentary, these solutions enabled wearers to continue their duties.

A significant turning point in prosthetic development occurred during the American Revolutionary War. It saw the introduction of the first artificial leg incorporating a rubber foot and ankle, enhancing comfort during wear **[1]**.

Another breakthrough emerged in the late 20th century with the use of composites in prosthetic manufacturing, resulting in lightweight and durable prosthetic legs and sockets. In 1984, Van Phillips created the "Flex-Foot" trans-tibial prosthetic using carbon graphite, marking the first prosthetic to store and release elastic energy during walking **[2]**.

Today, prosthetics continue to evolve, aiming to provide wearers with the most natural sensation possible. However, significant challenges persist.

This thesis focuses on studying lower limb running prosthetics. While running, the ankle and the Achilles tendon function like a spring, storing and releasing energy with each foot strike, as illustrated in **Fig. 1**. **[3]**.

Running prosthetics are designed based on this principle, explaining their departure from traditional prosthetic designs to adopt a "C" or "J" shape. The "C" shape benefits long-distance run-

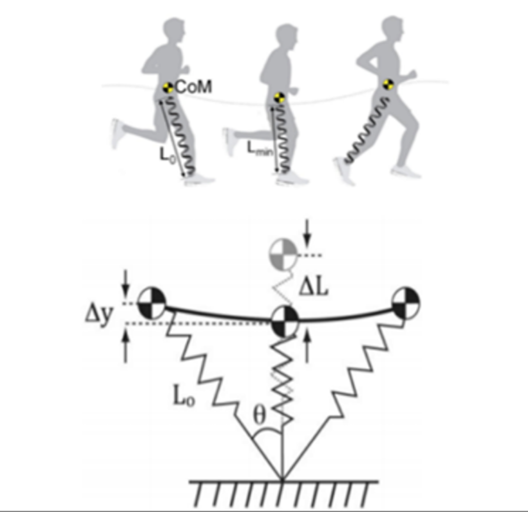


**Fig. 1.** *The ankle while running .*

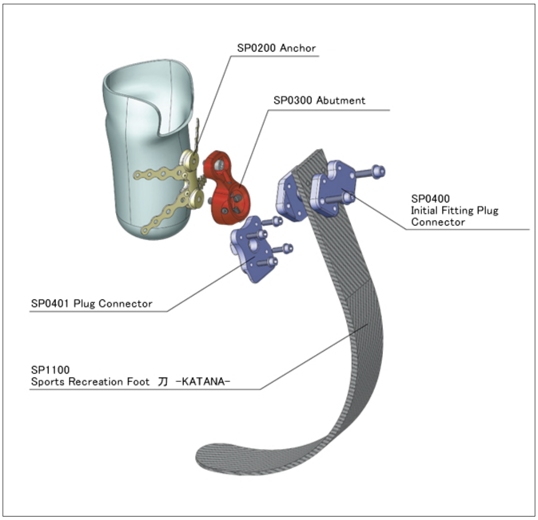


**Fig. 2.** *„J" shaped transtibial prostheses.*

ners, while the "J" shape favors sprinters due to greater release of elastic and mechanical energy, accelerating the runner in a shorter time. The latter design is depicted in **Fig. 2.** **[4]**.

As seen in the figure, the prosthetic foot is connected to the prosthetic socket through attachment components. The socket accommodates the residual limb and may be manufactured together with or separately from the prosthetic foot, depending on the manufacturer and prosthetic type. For runners, it is particularly important that the prosthesis be lightweight, yet strong and flexible, making material selection a critical factor. Carbon fiber composites are the most commonly used materials in running prostheses due to their exceptional strength and fatigue resistance relative to their weight. Carbon fiber-reinforced polymer (CFRP) and carbon fiber-reinforced nylon (CFRN) are frequently employed materials in prosthetic manufacturing.

The production of running prostheses is a time-consuming process that requires great attention to detail. After reinforcing and cutting the carbon fibers to the appropriate length, they are layered into a mold. The layers are bonded with resin, ensuring that no air bubbles remain between them. Depending on the manufacturer and type, 50–90 layers are stacked. Next, the layered structure, still in the mold, is placed in an autoclave, where it undergoes fusion at 150°C and 10 bar pressure. This process takes an average of two hours. Once cooled, a milling machine shapes the final form of the prosthetic limb. At this stage, the attachment components are also added, which will later connect the new foot to the socket of the residual limb. The finished product then undergoes multiple tests **[5]**.

Today, additive manufacturing offers the potential to significantly reduce production time, costs, and weight in prosthetic manufacturing. In 3D printing, several parameters can be adjusted. In this research, we aim to experiment with infill patterns. These patterns, ranging from simple lines to complex geometric structures, greatly influence printing time, material usage, and product flexibility. Different patterns vary in complexity and handle material differently. Depending on the intended application, it is crucial to carefully select the infill pattern**[6]**.

## 2. Research Objectives

The objectives of our research are as follows:

- –Investigating the additive manufacturing of prostheses;
- –Developing a transtibial running prosthesis model incorporating 3D-printable infill patterns;
- –Analyzing the load-bearing capacity of running prosthesis models with different infill patterns using the finite element method (FEM);
- –Identifying an optimal infill pattern that can be used in the additive manufacturing of transtibial running prostheses.

## 3. Theoretical Foundation

Our research consists of two main parts: design and testing. The design phase involves creating the transtibial running prosthesis model in Autodesk Inventor software. The foot design is based on the running prosthetic foot shown in Fig. 3.

The foot structure was based on the running blade shown in Figure 3. The advantage of the "J"-shaped running prosthesis is that the invested energy is recovered more efficiently and rapidly, allowing runners to achieve better performance in short-distance sprints. A key consideration in the design process is ensuring that the foot is lightweight while also providing stability for the user.

For the next phase, we created the model with an internal structure filled with different infill patterns that can be produced using additive manufacturing. In this study, we used a BCN3D Epsilon W50 printer, which has a printing volume of 420 × 300 × 400 mm and a precision of 1–1.25 µm. The printer is paired with the BCN3D Stratos software, which allows for the design and adjustment of manufacturing parameters. The printer features an Independent Dual Extruder (IDEX) system, which significantly reduces production time. It is capable of processing various materials, such as nylon, carbon fiber, PLA, and ABS filament.

The 3D printer we used can operate with fourteen different infill types. Since the prosthesis must be both lightweight and load-bearing, we selected the following infill patterns for experimentation: zig-zag, grid, tri-hexagon, and triangles (Table 1). These patterns were chosen due to their excellent load-bearing capacity, which remains relatively stable even when the infill density is modified. Infill density, like the pattern itself, significantly affects the quality of the final product. In this study, we aimed to keep the density constant in order to focus specifically on the effects of different infill patterns [8].

## 4. Practical Implementation

### 4.1. Design

In the first phase of our research, we designed a transtibial, J-shaped running prosthesis (Fig. 4). To minimize displacement under load, the prosthetic foot was designed using multiple circular arcs. During the design process, we observed that the size of the R2 arc is a critical factor influencing displacement (Fig. 3), as increasing its size results in greater deformation in this section. This may compromise the manageability of the prosthesis, reduce wearer comfort, and negatively affect its load-bearing capacity. A key design consideration was minimizing of the arc that contacts the ground to ensure optimal energy storage and release.

**Table 1.** *Grid, zig-zag, triangles infill patterns*

| | | |
|---|---|---|
| 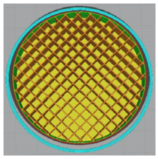 | 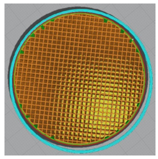 | 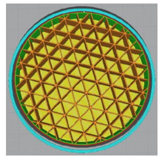 |
| Grid | Zig-zag | Triangles |

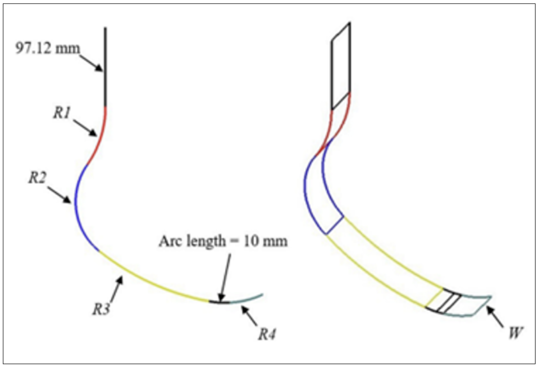


**Fig. 3.** *The prosthesis on which the design is based.* [7]

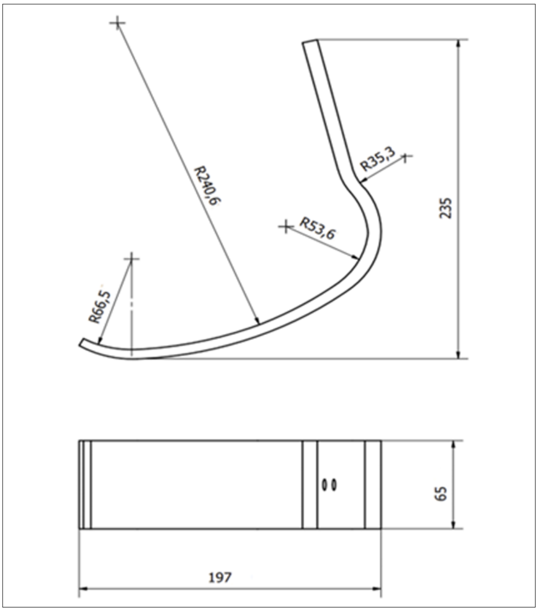


**Fig. 4.** *Design of the model.*

Following the creation of the initial sketch, the prosthesis model was developed using Autodesk Inventor Professional software. The first iteration featured a fully solid structure, serving as a reference point for subsequent analyses. The internal structure was then modified using different infill patterns.

The first infill pattern examined was the grid infill (Fig. 5). consisting of two-dimensional lines oriented in two perpendicular directions within each layer. This pattern provides a balance between material usage and print time efficiency. The design process considered the parameters of the 3D printer, particularly the nozzle diameters, which played a key role in determining line thickness (0.8 mm) and spacing (10 mm). This resulted in a relatively dense structure, ensuring sufficient load-bearing capacity while still being recognized as a hollow object by the testing software. To enhance the visibility of the infill's effects, the wall thickness was minimized to 1 mm, a value maintained consistently across all tested configurations.

The second infill pattern implemented was the triangles infill (Fig. 6), ), in which the internal lines are oriented in three directions within the XY plane. Similar to the previous pattern, the lines intersect within each layer, thereby reinforcing the structure. In terms of material consumption and printing time, the triangles infill is comparable to the grid pattern. Since it was not possible to directly adjust or analyze the infill density in the given software, parameters were selected to ensure approximately equivalent volume across different patterns. The volume achieved with the grid infill was 80 906.7 mm³, while the triangles pattern resulted in a volume of 77 435 mm³. In this case, parallel lines with a thickness of 0.4 mm were spaced 10 mm apart, intersecting at angles of 60°. The wall thickness was maintained at 1 mm.

The third infill pattern examined was the zig-zag infill (Fig. 7), which is structurally similar to the grid pattern but differs in a key aspect: in this configuration, the lines do not intersect within a single layer. Instead, the nozzle reverses direction upon reaching the outer wall, creating a continuous, interconnected structure. This design significantly reduces printing time compared to the other patterns. To achieve a comparable volume of 81 152.6 mm³, the line spacing was set to 10 mm, with a line thickness of 0.4 mm.

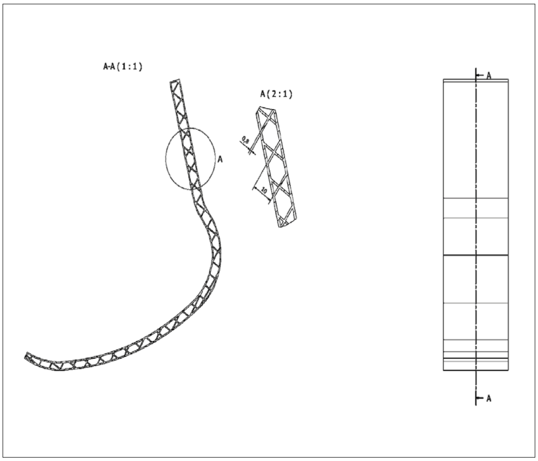


**Fig. 5.** *The grid infill pattern.*

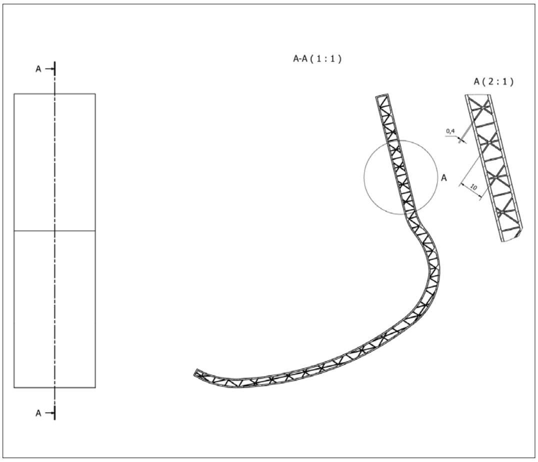


**Fig. 6.** *The grid infill pattern*

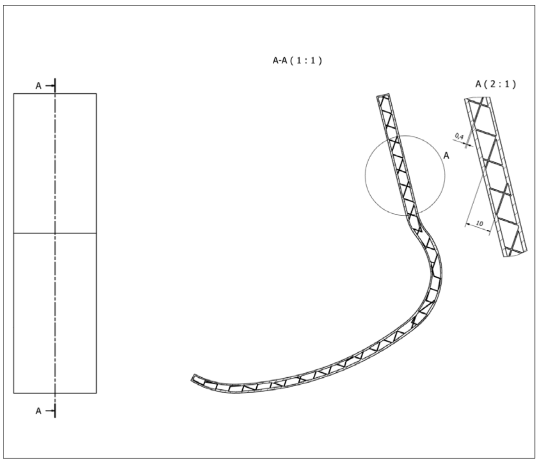


**Fig. 7.** *Zig-zag infill pattern.*

### 4.2. Testing

During the testing phase, the transtibial running prosthesis models with different infill patterns were analyzed using the finite element method in ANSYS software. The models were subjected to three distinct loads: 700 N, 1400 N, and 2100 N, corresponding to standing, walking, and running conditions, respectively [9]. These three load values were selected to provide a comprehensive understanding of the model's load-bearing capacity and limitations. The stress distribution and displacements within the model were examined and interpreted.

To achieve the highest possible accuracy, the model was subdivided into numerous triangular finite elements, forming a computational mesh. The selection of an appropriate mesh size is a critical aspect of finite element analysis: an excessively large mesh results in inaccurate outcomes, whereas an overly fine mesh may exceed the computational capacity of the available software. Therefore, a balance had to be struck between computational efficiency and precision.

The variation in Von Mises stress within the grid-infill prosthesis under a 2100 N load was analyzed by applying different mesh sizes (Fig. 8). As the mesh size increased, the stress value decreased, following a polynomial trend. This phenomenon likely occurs because larger elements fail to fully capture the internal pattern. Due to software limitations, a mesh size of 3.3 mm was selected to obtain the most precise results regarding the model's structural properties.

The model also included constraints at the region where the foot contacts the ground. The simulation software facilitated material selection, enabling the specification of the prosthesis material. Carbon Fiber-Reinforced Plastic (CFRP) was chosen, as it is widely used in the manufacturing of running prostheses due to its favorable properties: lightweight nature, high load-bearing capacity, and excellent fatigue resistance.

From a displacement perspective, flexibility is crucial; however, excessive deformation could lead to premature failure.

## 5. Results

### 5.1. Mass

The simulation software calculated the prosthesis mass based on its volume and material density. The fully solid model had a relatively low mass of 0.294 kg, but this was further reduced by incorporating infill patterns (Fig. 9). Since prosthetic users are highly sensitive to weight differences, minimizing the mass is a key design goal.

By using optimized infill patterns, the prosthesis mass was reduced to less than half of the original, with the triangles-infill prosthesis achieving the lowest mass of 0.111 kg. This represents a reduction of approximately 180 g, which, while seemingly minor, translates to a 60% material savings, making the manufacturing process both more efficient and cost-effective.

### 5.2. Total displacement

Next, the reaction of different infill-patterned prostheses to applied loads was analyzed. Under loading, various regions of the model undergo displacement relative to their original positions, depending on the force direction and the constraint conditions. In this study, a vertically directed force was applied to the prosthesis' upper section, while the lower part was fixed. This led to the greatest displacement occurring in the upper region of the prosthesis.

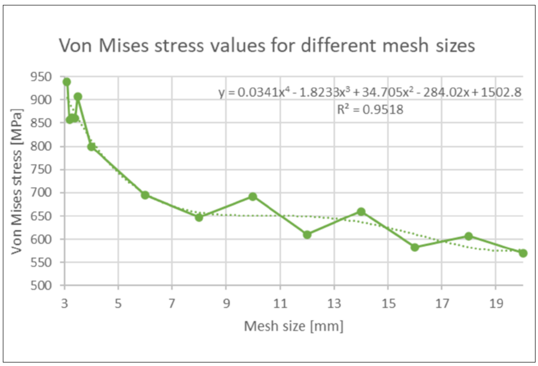


**Fig. 8.** *Von Mises stress values for different mesh sizes.*

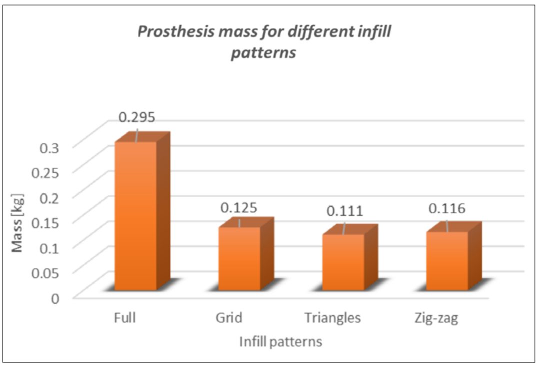


**Fig.9.** *Prosthesis mass for different infill patterns*

The deformation increased linearly with the applied load (Fig. 10). The displacement grew more rapidly for infill-patterned prostheses compared to the fully solid model.

At low loads, the displacement values for all infill-patterned prostheses were nearly identical, with minimal variation. At maximum load, some divergence was observed, though the differences remained relatively small. The zig-zag infill pattern exhibited the smallest displacement at maximum load (d = 14.5 mm), while the triangles pattern resulted in the largest displacement (d = 17.1 mm). This was more than 1.5 times the deformation of the fully solid model (d = 10 mm).

The grid and triangles patterns exhibited nearly identical deformation behavior across all load cases.

A maximum deformation limit of 50 mm was set, ensuring structural integrity while allowing for an observable deformation response [10]. None of the models exceeded this threshold, even under the highest applied load. Since greater deformation enhances energy storage and return, the use of optimized infill patterns can improve the prosthesis' energy efficiency.

### 5.3. Von Mises Stress Analysis

The increase in stress values followed a linear trend with respect to applied load (Fig. 11). The fully solid model exhibited a gradual increase in Von Mises stress, reaching 494 MPa at maximum load. In contrast, the infill-patterned models demonstrated a steeper stress increase.

For the triangles and grid infill patterns, similar stress values were observed at all load levels. The triangles pattern exhibited a slight reduction in stress, remaining approximately 30 MPa lower than the grid pattern under maximum load.

The zig-zag infill pattern resulted in the highest stress values, reaching 377 MPa under a 700 N load and increasing rapidly to 1130 MPa at a 2100 N load.

CFRP is a high-performance polymer with an ultimate tensile strength of 1100 MPa [11]. Generally, if the Von Mises stress exceeds this threshold, material failure is likely. Based on the analysis, the grid and triangles infill patterns remained within safe stress limits even under maximum load, whereas the zig-zag pattern exceeded 1130 MPa, indicating potential failure.

## 6. Conclusions

Based on the results, we can conclude that parts manufactured with infill patterns do not offer the same load bearing capacity as the fully filled model. They exhibit greater deformation under load, and their structural integrity is significantly reduced. However, the findings suggest that the triangles and grid infill patterns offer promising solutions for the additive manufacturing of running prostheses. These patterns not only enable weight reduction and material savings but also provide sufficient resistance to loads and possess favorable energy storage properties. This opens up opportunities for future research to develop lighter, more cost-effective, and customized running prostheses.

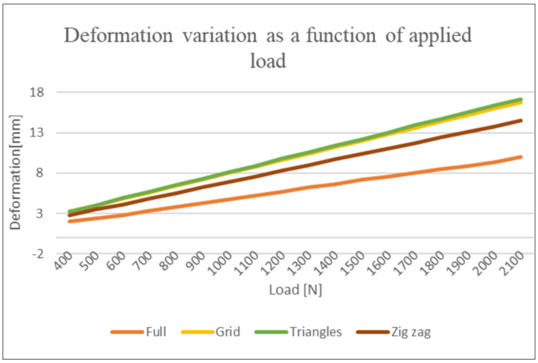


**Fig. 10.** *Deformation variation as a function of applied load.*

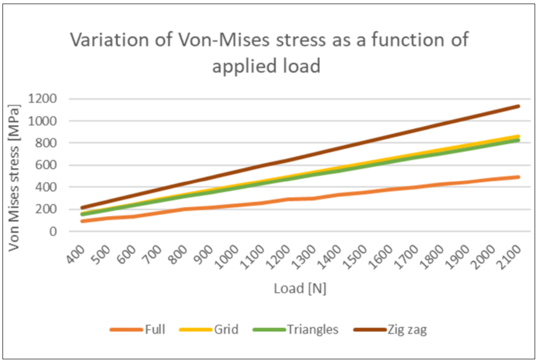


**Fig. 11.** *Variation of Von-Mises stress as a function of applied load.*

### References

[1] NIH Medline Plus Mgazine. Prosthetics through the Ages. (megtekintve: 2024. 12. 12. https://magazine.medlineplus.gov/article/prosthetics-through-the-ages)

[2] Hobara H.: *Running-Specific Prostheses: The History, Mechanics, and Controversy*. Journal of the Society of Biomechanisms, 38. (2014) 105–110.

https://www.jstage.jst.go.jp/article/sobim/38/2/38_105/_pdf (letöltve: 2023. 11. 15.)

[3] Martín-Sacristán, A.L.: *Biomechanical Model to Optimize Unilateral Blade Running*. TU Delft Repositories, 2021. (letöltve: 2023. 12. 05.) https://repository.tudelft.nl/islandora/object/uuid%3Aff408e81-f996-4914-9bd4-4b1cfc78b401

[4] Imasen Engineering Coorporation, Lapoc Sports Samuray Assembly. (megtekintve: 2023.11.15.) https://www.imasengiken.co.jp/en/lapoc/sport.html

[5] National Paralympic Heritage Trust. Running Blades and Their Evolution. https://www.paralympicheritage.org.uk/running-blades-and-their-evolution

[6] Akhoundi, B., Behravesh, A.H.: *Effect of Filling Pattern on the Tensile and Flexural Mechanical Properties of FDM 3D Printed Products*. Experimental Mechanics, 59. (2019) 883–897 https://doi.org/10.1007/s11340-018-00467-y

[7] Solis, M.J.R., Ramírez, J.O.D., Salazar, J.M., Ochoa, J.A.R., Roa, A.G.: *Optimization of Running Blade Prosthetics Utilizing Crow Search Algorithm Assisted by Artificial Neural Networks*. Journal of Mechanical Engineering, 67. (2021) 88–100. https://doi.org/10.5545/sv-jme.2020.6990

[8] Perneta, B., Nagelb, J.K., Zhang, H.: *Compressive Strength Assessment of 3D Printing Infill Patterns*. Procedia CIRP, 105. (2022) 682–687. https://doi.org/10.1016/j.procir.2022.02.114

[9] Siddiqui, I.H., Arifudin, L., Alnaser, I.A., Hassan, A., Alluhydan, K.: *Static Behavior of a Prosthetic Running Blade Made from Alloys and Carbon Fiber*. Journal of Disability Research, 2/1. (2023) 63–74. https://doi.org/10.57197/JDR-2023-0010

[10] Tip Composite. CFRP Specification. (megtekintve: 2025.02.06.) https://tip-composite.com/en/product-information/cfrp/cfrp-specification/

[11] Élodie Doyen, Fabien Szmytka, Jean-François Semblat: *A Novel Characterisation Protocol of Mechanical Interactions between the Ground and a Tibial Prosthesis for Long Jump*. Scientific Reports, 13. (2023) 5226. https://doi.org/10.1038/s41598-023-31981-2